Anisotropic Polyethylene Nanocrystals Labeled with a Single Fluorescent Dye Molecule: Towards Monitoring of Nanoparticle Orientation

Benjamin Scheinhardt,[†,‡] Justyna Trzaskowski,[†] Moritz C. Baier,[†] Beate Stempfle,[†] Alex Oppermann,[†] Dominik Wöll,[*,†,‡,§] and Stefan Mecking[*,†,‡]

[†] Department of Chemistry, University of Konstanz, Universitätsstrasse 10, 78457 Konstanz, Germany

[‡] Konstanz Research School Chemical Biology, University of Konstanz, Universitätsstrasse 10, 78457 Konstanz, Germany

[§] Zukunftskolleg, University of Konstanz, Universitätsstrasse 10, 78457 Konstanz. Germany

Tel: +49 7531 88 5151, Email: stefan.mecking@uni-konstanz.de

SUPPORTING INFORMATION

1. Defocused widefield fluorescence microscopy S2
2. Synthesis of fluorescence functionalized ROMP initiator **1**.....S3-S9
3. Initiation kinetics of initiator **1** S10-S11
4. Synthesis of single labeled PE nanocrystals.....S12-S16
5. AFM studies.....S17-S19
6. Defocused widefield images.....S20-S22

1. Defocused widefield fluorescence microscopy

For excitation of the dyes, the beam of a diode-pumped solid state laser (561 nm, Cobolt Jive, 100 mW) was magnified by two lenses (f_1 = 40 mm and f_2 = 200 mm). This beam was sent onto a mirror (angle 45°) and through a third lens (Köhler illumination). Lens and mirror where mounted on a translation stage. If the stage is moved perpendicular to the beam path, the beam leaves the optical axis and enters the objective (Leica 100x oil immersion objective, 1.25 NA) no longer in the center. If a sample with an interface (here: glass/polymer) is placed onto the microscope, and the incident angle of the beam at the interface is at or below the so-called critical angle, total internal reflection occurs. However, with the 1.25 NA objective used in this work, it was not possible to achieve complete reflection of the laser beam, but only of a part of it. This is known as 'quasi total internal reflection mode' (qTIRF). This mode is sufficient for a good excitation of dye molecules of various orientations. The emission pattern observed only depends on the orientation of the transition dipole moment of the dye molecule with respect to the optical axis of the microscope. Inhomogeneities or polarization effects of the excitation light only change the intensity of the emission signal, but not its pattern.

The fluorescence light was collected with the same objective, separated from the excitation light by a trichroic mirror (z405/561/657rpc, AHF Analysentechnik), further magnified by two photo objectives (Nikkor) and imaged onto the chip of a CCD-camera (Andor iXon+). To enhance the S/N-ratio, a notch filter (E grade, 561 nm, AHF) and a bandpass filter (Brightline HC 617/73, AHF) were placed between the photo objectives and a clean-up filter (z561/10, AHF) was positioned in front of the laser. The total magnification was 300-fold, resulting in an image with 53 nm per pixel. All measurements were performed at 293 K. Defocused images were obtained by positioning the sample ~1 µm towards the microscope objective from the focus using a piezoelectric transducer (P-545.xR7, Physik Instrumente). Integration times per frame varied between 30 and 200 ms.

2. Synthesis of fluorescence functionalized ROMP initiator 1

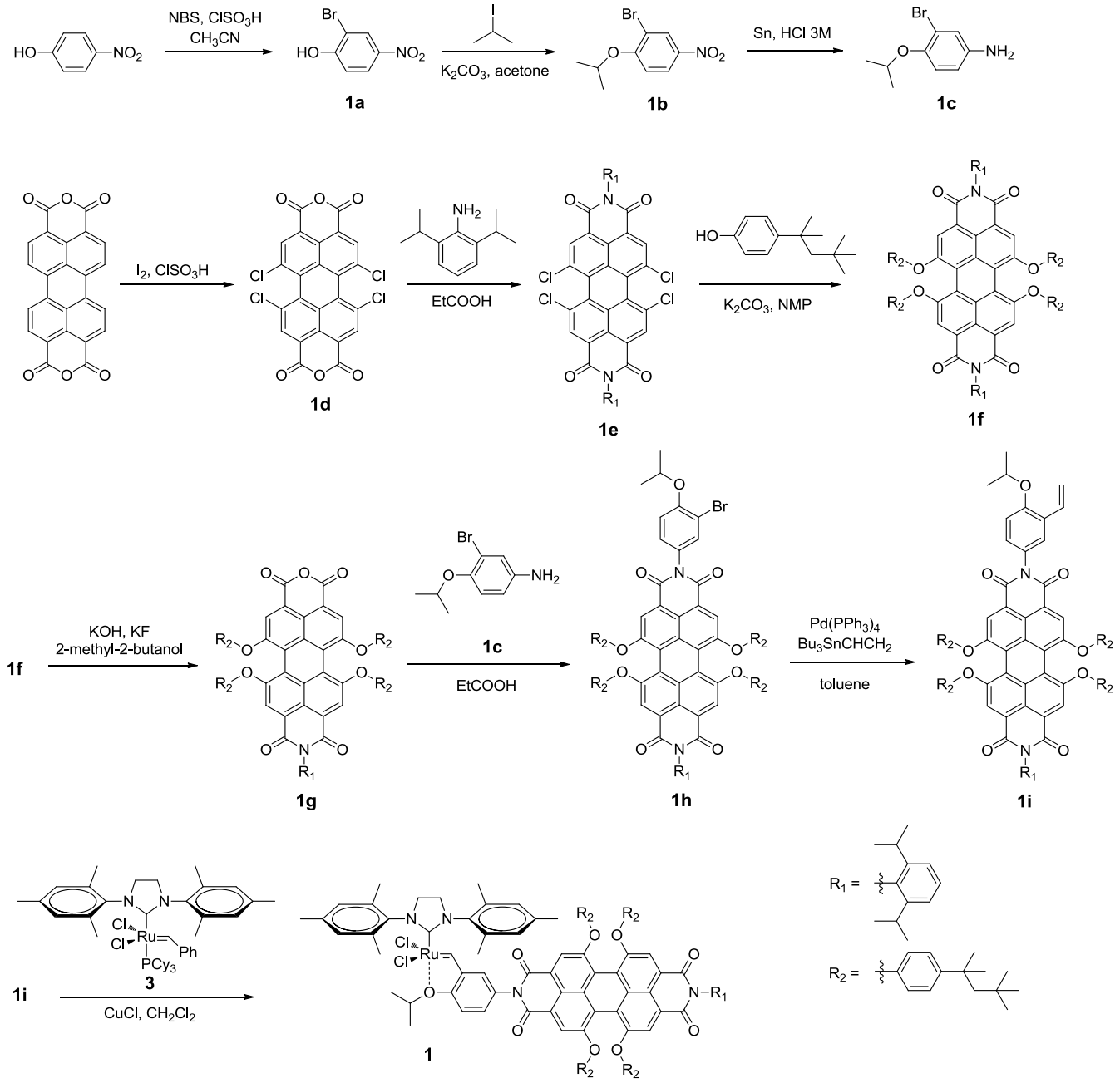

Figure S1. Synthesis of initiator **1**.

2-Bromo-4-nitrophenol 1a.[S1]

4-Nitrophenol (10.0 g, 71.89 mmol) in 100 mL dry CH_3CN was cooled to -30 °C under argon. Chlorosulfonic acid (9.2 g, 78.9 mmol) and NBS (15.3 g, 85.9 mmol) were added and the mixture was kept at -30 °C for another 0.5 h. Upon warming to room temperature the reaction mixture was stirred for 48 h. Subsequently, 100 mL 25 % Na_2SO_3 (aq) were added and the mixture was extracted with diethyl ether (2 x 150 mL). The combined organic phase was washed with water (3 x 100 mL) and brine (150 mL), dried over $MgSO_4$ and concentrated under reduced pressure. The brownish solid was subjected to column chromatography on silica gel with ethyl acetate/pentane (1:4) as eluent to yield 8.6 g of a yellow solid (55 %).

^{1}H-NMR (400 MHz, $CDCl_3$, 25 °C) δ 8.44 (d, J = 2.60 Hz, 1H, phenylic *H* ortho to Br), 8.17 (dd, J = 9.05, 2.60 Hz, 1H, phenylic *H* para to Br), 7.14 (d, J = 9.05 Hz, 1H, phenylic *H* ortho to OH), 6.15 (bs, 1H, O*H*).

2-Bromo-1-isopropoxy-4-nitrobenzene 1b.[S2]

To a solution of 2-bromo-4-nitrophenol **1a** (8.0 g, 36.7 mmol) in 120 mL dry acetone under argon were added K_2CO_3 (10.1 g, 73.4 mmol) and isopropyl iodide (12.5 g, 73.4 mmol). The resulting mixture was stirred at reflux for 48 h. Upon cooling to room temperature ethyl acetate (150 mL) and a saturated solution of sodium hydrocarbonate (100 mL) were added. The aqueous layer was extracted with ethyl acetate (1 x 100 mL) and the combined organic phase was washed with a saturated solution of sodium hydrocarbonate (2 x 100 mL), brine (1 x 100 mL), dried over $MgSO_4$ and concentrated under reduced pressure. The yellow oil was recrystallized from ethanol to yield 7.0 g of a pale yellow solid (74 %).

^{1}H-NMR (400 MHz, $CDCl_3$, 25 °C) δ 8.47 (d, J = 2.77 Hz, 1H, phenylic *H* ortho to Br), 8.18 (dd, J = 9.14, 2.77 Hz, 1H, phenylic *H* para to Br), 6.94 (d, J = 9.14 Hz, 1H, phenylic *H* ortho to $OCHMe_2$), 4.72 (sept, J = 6.04 Hz, 1H, $PhOC\mathit{H}Me_2$), 1.45 (d, J = 6.04 Hz, 6H, $PhOCH(C\mathit{H}_3)_2$).

3-Bromo-4-isopropoxyaniline 1c.[S2]

To a solution of 2-bromo-1-isopropoxy-4-nitrobenzene **1b** (6.9 g, 26.8 mmol) in 140 mL 3M HCl (aq) was added tin (4.8 g, 40.1 mmol) at room temperature. The mixture was heated to reflux for 3.5 h. Upon cooling to room temperature the solution was poured into 600 mL 1M NaOH (aq) and the mixture was extracted with ethyl acetate (8 x 190 mL). The organic phase was washed with brine (1 x 400 mL), dried over $MgSO_4$ and concentrated under reduced pressure to afford a brown oil. Column chromatography on silica gel with ethyl acetate/pentane (1:4) yielded 3.47 g of a brown oil (56 %).

^{1}H-NMR (400 MHz, $CDCl_3$, 25 °C) δ 6.91 (d, J = 2.77 Hz, 1H, phenylic *H* ortho to Br), 6.79 (d, J = 8.63, 1H, phenylic *H* ortho to $OCHMe_2$), 6.57 (dd, J = 8.63 Hz, 2.77 Hz, 1H, phenylic *H* para to Br), 4.33 (sept, J = 6.04 Hz, 1H, PhOC*H*Me_2), 3.39 (bs, 2H, NH_2), 1.33 (d, J = 6.04 Hz, 6H, PhOCH(CH_3)$_2$).

1,6,7,12-Tetrachloroperylene-3,4,9,10-tetracarboxylic dianhydride 1d.[S3]

3,4,9,10-Perylentetracarboxylic dianhydride (10.0 g, 25.5 mmol) and iodine (1.72 g, 6.8 mmol) were stirred in 60 mL chlorosulfonic acid for 21 h at 70 °C. Upon cooling to room temperature, the reaction mixture was poured very slowly in 700 mL of a stirred ice/water mixture. The red precipitate was filtered off with a glass frit and washed with water. Drying at 50 °C in vacuo yielded 16.1 g of an orange powder. The product was used without further purification.

^{1}H-NMR (400 MHz, $CDCl_3$, 25 °C) δ 8.75 (s, 4H, perylene *H*).

N,N'-Bis(2,6-diisopropylphenyl)-1,6,7,12-tetrachloroperylene-3,4,9,10-tetracarboxylic diimide 1e.[S4]

1,6,7,12-Tetrachloroperylene-3,4,9,10-tetracarboxylic dianhydride **1d** (4.0 g, 7.5 mmol) and 2,6-diisopropylaniline (5.3 g, 30.0 mmol) were refluxed in 240 mL of propionic acid under an argon atmosphere for 17 h at 150 °C. Upon cooling to room temperature the reaction mixture was poured into

1.3 L of water. The red precipitate was filtered off and washed with water. Column chromatography on silica gel with CH_2Cl_2 as eluent yielded 5.1 g (6.0 mmol) of a red-orange solid (80 % yield).

^{1}H-NMR (400 MHz, CD_2Cl_2, 25 °C) δ 8.77 (s, 4H, perylene *H*), 7.55 (t, J = 7.82 Hz, 2H, phenylic *H* para to N), 7.39 (d, J = 7.82 Hz, 4H, phenylic *H* meta to N), 2.75 (sept, J = 6.79 Hz, 4H, PhC*H*Me_2), 1.16 (t, J = 6.79 Hz, 24H, C*H*$_3$).

N,N'-Bis(2,6-diisopropylphenyl)-1,6,7,12-tetra[4-(1,1,3,3-tetramethylbutyl)phenoxy]-perylene-3,4,9,10-tetracarboxylic diimide 1f.[S4]

N,N'-Bis(2,6-diisopropylphenyl)-1,6,7,12-tetrachloroperylene-3,4,9,10-tetracarboxylic diimide **1e** (3.0 g, 3.5 mmol), tert-octylphenol (3.6 g, 17.5 mmol) and K_2CO_3 (1.2 g, 8.75 mmol) were stirred in 60 mL NMP for 60 h at 140 °C under an argon atmosphere. Upon cooling to room temperature the reaction mixture was poured into a mixture of 100 mL 10 % HCl and 150 mL MeOH. The purple precipitate was filtered off, washed with 200 mL of H_2O/MeOH (2:3) and dried at 50 °C under vacuum. Column chromatography on silica gel with CH_2Cl_2 / petroleum ether (1:2) as eluent yielded 3.3 g of a red solid (62 % yield).

^{1}H-NMR (400 MHz, CD_2Cl_2, 25 °C) δ 8.12 (s, 4H, perylene *H*), 7.45 (t, J = 7.88 Hz, 2H, phenylic *H* para to N), 7.36 (d, J = 8.78 Hz, 8H, phenylic *H* meta to O), 7.30 (d, J = 7.88 Hz, 4H, phenylic *H* meta to N), 6.95 (d, J = 8.78 Hz, 8H, phenylic *H* ortho to O), 2.69 (sept, J = 6.87 Hz, 4H, NPhC*H*Me_2), 1.74 (s, 8H, C*H*$_2$CMe_3), 1.37 (s, 24H, OPhC(C*H*$_3$)$_2$), 1.09 (d, J = 6.87 Hz, 24H, NPhCH(C*H*$_3$)$_2$), 0.76 (s, 36H, C(C*H*$_3$)$_3$).

N-(2,6-Diisopropylphenyl)-1,6,7,12-tetra[4-(1,1,3,3-tetramethylbutyl)phenoxy]-perylenetetracarboxylic-3,4-anhydride-9,10-imide 1g.[S5]

N,N'-Bis(2,6-diisopropylphenyl)-1,6,7,12-tetra[4-(1,1,3,3-tetramethylbutyl)phenoxy]-perylene-3,4,9,10-tetracarboxylic diimide **1f** (1.2 g, 0.79 mmol) in 19 mL 2-methyl-2-butanol was heated to

60 °C under an argon atmosphere. After 0.5 h KOH (1.32 g, 23.6 mmol) and KF (1.37 g, 23.6 mmol) were added and the mixture was stirred at 80 °C for 72 h. The reaction mixture was cooled to 50 °C and 24 mL 50 % AcOH (aq) were added. Upon stirring for another 2 h at 80 °C the mixture was cooled to room temperature and poured into 400 mL of water. The red precipitate was filtered off, washed with 500 mL hot water and dried at 50 °C under vacuum. Column chromatography on silica gel with CH_2Cl_2 / pentane (1:1) as eluent yielded 418 mg of a dark red solid (39 %).

^{1}H-NMR (400 MHz, CD_2Cl_2, 25 °C) δ 8.11 (s, 2H, perylene *H*), 8.09 (s, 2H, perylene *H*), 7.45 (t, J = 7.75 Hz, 1H, phenylic *H* para to N), 7.37 (d, J = 7.70 Hz, 4H, phenylic *H* meta to O), 7.35 (d, J = 7.70 Hz, 4H, phenylic *H* meta to O), 7.30 (d, J = 7.75 Hz, 2H, phenylic *H* meta to N), 6.94 (d, J = 3.36 Hz, 4H, phenylic *H* ortho to O), 6.92 (d, J = 3.36 Hz, 4H, phenylic *H* ortho to O), 2.67 (sept, J = 6.76 Hz, 2H, NPhC*H*Me_2), 1.77 (s, 4H, CH_2CMe_3), 1.74 (s, 4H, CH_2CMe_3), 1.39 (s, 12H, OPhC(CH_3)$_2$), 1.36 (s, 12H, OPhC(CH_3)$_2$), 1.09 (d, J = 6.76 Hz, 12H, NPhCH(CH_3)$_2$), 0.79 (s, 18H, C(CH_3)$_3$), 0.75 (s, 18H, C(CH_3)$_3$).

N-(2,6-Diisopropylphenyl)-N'-(3-bromo-4-isopropoxyphenyl)-1,6,7,12-tetra[4-(1,1,3,3-tetramethylbutyl)phenoxy]-perylene-3,4,9,10-tetracarboxylic diimide 1h.

N-(2,6-Diisopropylphenyl)-1,6,7,12-tetra[4-(1,1,3,3-tetramethylbutyl)phenoxy]-perylenetetracarboxylic-3,4-anhydride-9,10-imide **1g** (195 mg, 143 µmol) and 3-Bromo-4-isopropoxyaniline **1c** (328 mg, 1.43 mmol) in 14 mL propionic acid were heated to 140 °C for 2 h under an argon atmosphere. Upon cooling to room temperature the reaction mixture was poured into 100 mL of water. The red precipitate was filtered off, washed with water and dried at 50 °C under vacuum. Column chromatography on silica gel with CH_2Cl_2 / hexane (1:1) as eluent yielded 190 mg of a dark red solid (84 %).

^{1}H-NMR (400 MHz, CD_2Cl_2, 25 °C) δ 8.12 (s, 2H, perylene *H*), 8.12 (s, 2H, perylene *H*), 7.45 (t, J = 7.80 Hz, 1H, phenylic *H* para to N), 7.43 (d, J = 2.56 Hz, 1H, phenylic *H* ortho to Br), 7.34 (d,

J = 8.77 Hz, 4H, phenylic *H* meta to O), 7.34 (d, J = 8.77 Hz, 4H, phenylic *H* meta to O), 7.30 (d, J = 7.80 Hz, 2H, phenylic *H* meta to N), 7.16 (dd, J = 8.82, 2.56 Hz, 1H, phenylic *H* para to Br), 7.04 (d, J = 8.82 Hz, 1H, phenylic *H* ortho to $OCHMe_2$), 6.93 (d, J = 8.77 Hz, 4H, phenylic *H* ortho to O), 6.93 (d, J = 8.77 Hz, 4H, phenylic *H* ortho to O), 4.63 (sept, J = 6.04 Hz, 1H, $PhOC\mathit{H}Me_2$), 2.69 (sept, J = 6.78 Hz, 2H, $NPhC\mathit{H}Me_2$), 1.75 (s, 4H, $C\mathit{H}_2CMe_3$), 1.73 (s, 4H, $C\mathit{H}_2CMe_3$), 1.42 (d, J = 6.04 Hz, 6H, $PhOCH(C\mathit{H}_3)_2$), 1.36 (s, 24H, $OPhC(C\mathit{H}_3)_2$), 1.09 (d, J = 6.78 Hz, 12H, $NPhCH(C\mathit{H}_3)_2$), 0.77 (s, 18H, $C(C\mathit{H}_3)_3$), 0.75 (s, 18H, $C(C\mathit{H}_3)_3$).

N-(2,6-Diisopropylphenyl)-N'-(3-vinyl-4-isopropoxyphenyl)-1,6,7,12-tetra[4-(1,1,3,3-tetramethylbutyl)phenoxy]-perylene-3,4,9,10-tetracarboxylic diimide 1i.

N-(2,6-Diisopropylphenyl)-N'-(3-bromo-4-isopropoxyphenyl)-1,6,7,12-tetra[4-(1,1,3,3-tetramethylbutyl)phenoxy]-perylene-3,4,9,10-tetracarboxylic diimide **1h** (180 mg, 114 µmol) and Tributyl(vinyl)stannane (180 mg, 568 µmol) were dissolved in 9 mL of dry toluene and the solution was degassed several times. Tetrakis(triphenylphosphine)palladium (67.5 mg, 58 µmol) was added and the mixture was heated to 110 °C for 18 h. Upon cooling to room temperature the solvent was evaporated and the crude product was purified by column chromatography on silica gel with CH_2Cl_2 / hexane (1:1) as eluent to yield 137 mg of a dark red solid (79 %).

^{1}H-NMR (400 MHz, CD_2Cl_2, 25 °C) δ 8.13 (s, 2H, perylene *H*), 8.12 (s, 2H, perylene *H*), 7.45 (t, J = 7.80 Hz, 1H, phenylic *H* para to N), 7.34 (d, J = 8.77 Hz, 4H, phenylic *H* meta to O), 7.34 (d, J = 8.77 Hz, 4H, phenylic *H* meta to O), 7.30 (d, J = 7.80 Hz, 2H, phenylic *H* meta to N), 7.10 – 6.98 (m, 4H, $NC_6\mathit{H}_3O^iPrC\mathit{H}CH_2$), 6.94 (d, J = 8.77 Hz, 4H, phenylic *H* ortho to O), 6.93 (d, J = 8.77 Hz, 4H, phenylic *H* ortho to O), 5.70 (dd, J = 17.70 Hz, 1.33 Hz, 1H, vinylic $C\mathit{H}H'$), 5.26 (dd, J = 11.23 Hz, 1.33 Hz, 1H, vinylic $CH\mathit{H}'$), 4.62 (sept, J = 6.19 Hz, 1H, $PhOC\mathit{H}Me_2$), 2.69 (sept, J = 6.76 Hz, 2H, $NPhC\mathit{H}Me_2$), 1.74 (s, 4H, $C\mathit{H}_2CMe_3$), 1.73 (s, 4H, $C\mathit{H}_2CMe_3$), 1.40 (d, J = 6.19 Hz, 6H,

PhOCH(CH_3)$_2$), 1.36 (s, 24H, OPhC(CH_3)$_2$), 1.09 (d, J = 6.76 Hz, 12H, NPhCH(CH_3)$_2$), 0.76 (s, 18H, C(CH_3)$_3$), 0.74 (s, 18H, C(CH_3)$_3$).

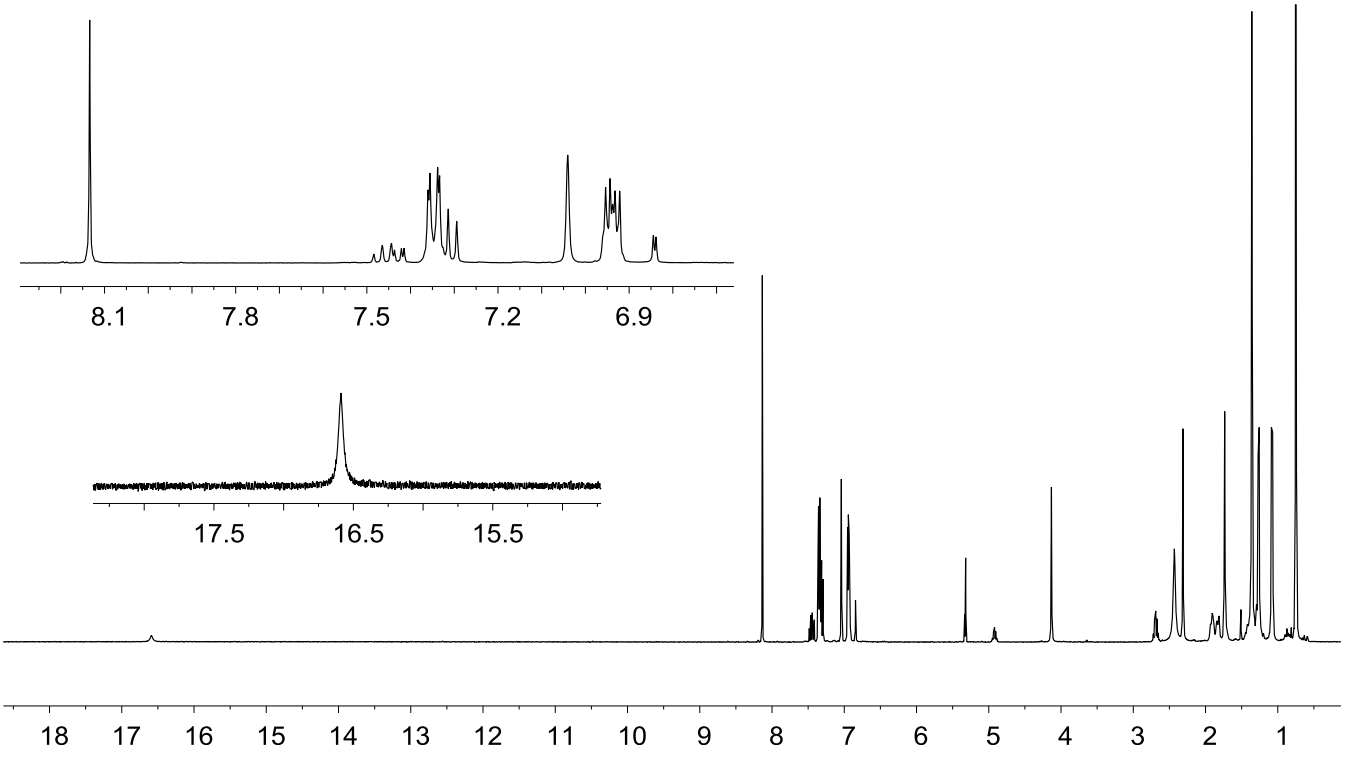

Figure S2. ^{1}H-NMR spectrum of fluorescence functionalized ROMP initiator **1** (25 °C, CD_2Cl_2).

3. Initiation kinetics of initiator 1

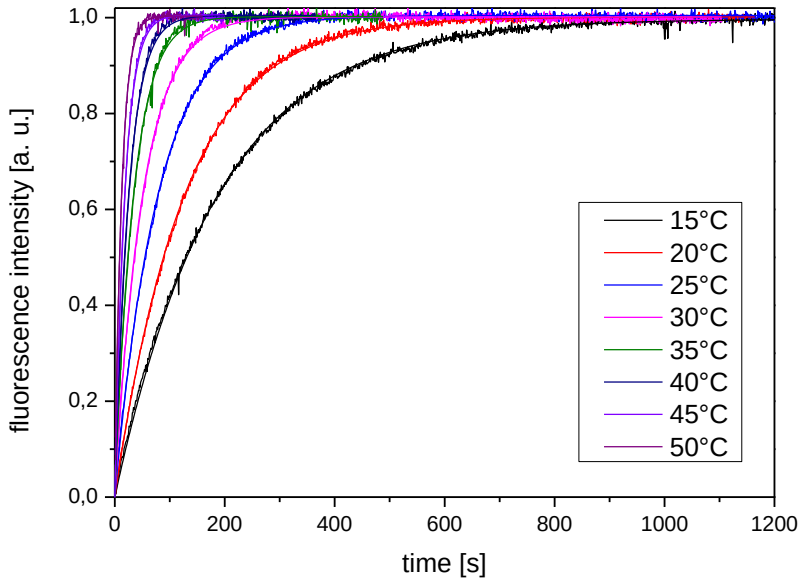

Figure S3. Increase in fluorescence intensity over time at λ = 619 nm in the reaction of **1** (1.9×10^{-5} mol L^{-1}) with n-butyl vinyl ether (0.15 mol L^{-1}) in toluene at various temperatures.

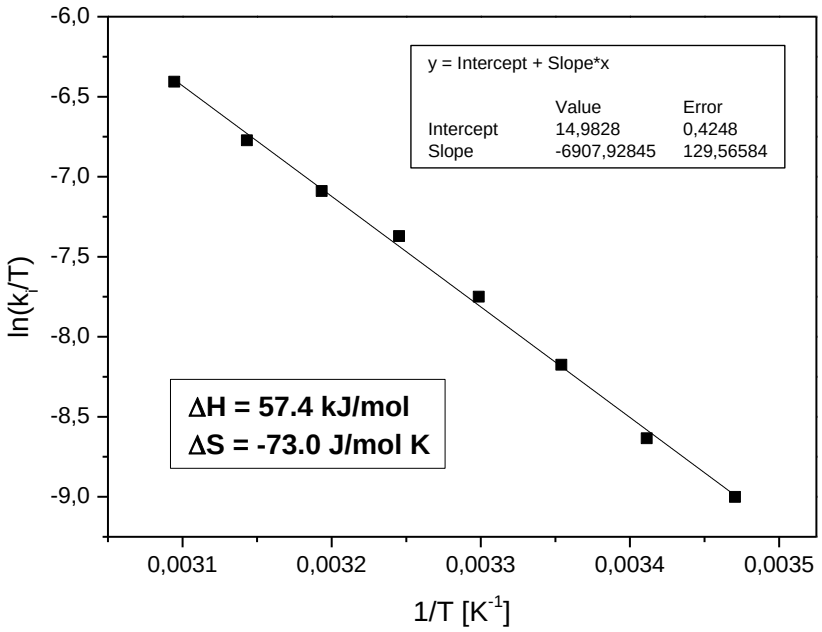

Figure S4. Eyring-plot for the initiation of **1** (1.9×10^{-5} mol L^{-1}) in the reaction with n-butyl vinyl ether (0.15 mol L^{-1}) in toluene.

Table S1. Activation energies and entropies for the initiation of metathesis ruthenium alkylidenes with n-butyl vinyl ether.

	$\Delta H^{\ddagger}$ [kJ mol^{-1}]	$\Delta S^{\ddagger}$ [J mol^{-1} K^{-1}]
2[S6]	63.6	-80,8
1[a]	57.4	-73.0

a) reaction with n-butyl vinyl ether (0.15 mol L^{-1}) in toluene.

The toluene solutions of dye labeled alkylidene initiator **1** exhibited a weak fluorescence due to low-level impurities of free dye. The intensity of this fluorescence signal at 619 nm was determined each time prior to the addition of n-butyl vinyl ether, and was subtracted from the resulting fluorescence intensities. Initiation rates k_i were calculated from a pseudo first order fit (eq 1) of the normalized fluorescence intensity increase over time, followed by a division of the k_{obs} value by the n-butyl vinyl ether concentration (eq 2).

$$[\mathrm{PDI}] = [\mathrm{Ru}]_{\mathrm{tot}} \cdot \left(1 - \exp(-k_{\mathrm{obs}} \cdot t)\right) \qquad \text{(eq 1)}$$

$$k_i = \frac{k_{\mathrm{obs}}}{[\mathrm{nBuOVinyl}]} \qquad \text{(eq 2)}$$

Activation energies and entropies were calculated from an Eyring plot.

4. Synthesis of single labeled PE nanocrystals

In order to confirm complete initiation of **1** under the conditions applied during the aqueous microemulsion polymerization process, an excess (~ 1 mL) of ethyl vinyl ether was added to the polymer dispersion after full monomer consumption. Upon stirring for 1 h at room temperature the polymer was precipitated in 300 mL acetone, filtered off, washed with acetone and dried under vacuum. 50 mg of the light red polymer were dissolved in 2 mL CH_2Cl_2, precipitated in 200 mL acetone and filtered off. Neither discoloration of the polymer nor coloration of the filtrate was observed after repeating this procedure three times. The solvent of the combined filtrate was removed under reduced pressure and no free dye was observed.

As a control experiment, 50 mg of the polymer were dissolved in 2 mL CH_2Cl_2 and 0.09 mg of **1** (1.8×10^{-5} mol L^{-1}, corresponding to monomer/initiator = 10,000) dissolved in 0.5 mL CH_2Cl_2 were added to this solution. Upon stirring for 20 min an excess (~ 1 mL) of ethyl vinyl ether was added and the solution was stirred for another 1 h. The polymer was precipitated in acetone, filtered off, redissolved in CH_2Cl_2 and reprecipitated in acetone. The combined, light red filtrate was concentrated under reduced pressure to yield free PDI dye.

To assess the required ratio of initiators **1** and **2** to obtain single dye labeled nanoparticles the number of polymer chains per nanocrystal N_{chains} was roughly estimated by assuming spherical particles (eq 3).

$$N_{\text{chains}} = \frac{4 \cdot \pi \cdot r^3 \cdot \rho_{\text{PE}} \cdot N_A}{3M} \qquad \text{(eq 3)}$$

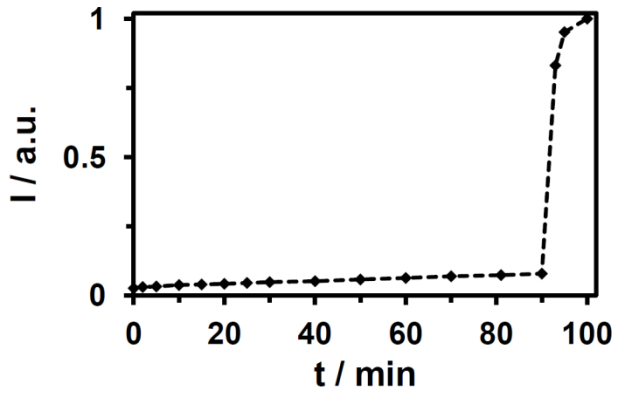

Figure S5. Fluorescence intensity of an aqueous microemulsion of initiator **1** at 20 °C over time, addition of ^{tr}COE microemulsion after 90 min.

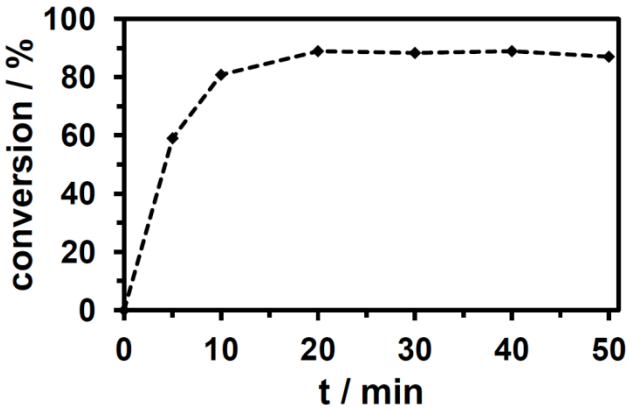

Figure S6. Conversion of ^{tr}COE during an aqueous microemulsion polymerization over time determined by precipitating aliquots after defined time intervals in MeOH (initiator **1**, mon./cat. = 20,000, 20 °C), indicating complete reaction after ~ 20 min.

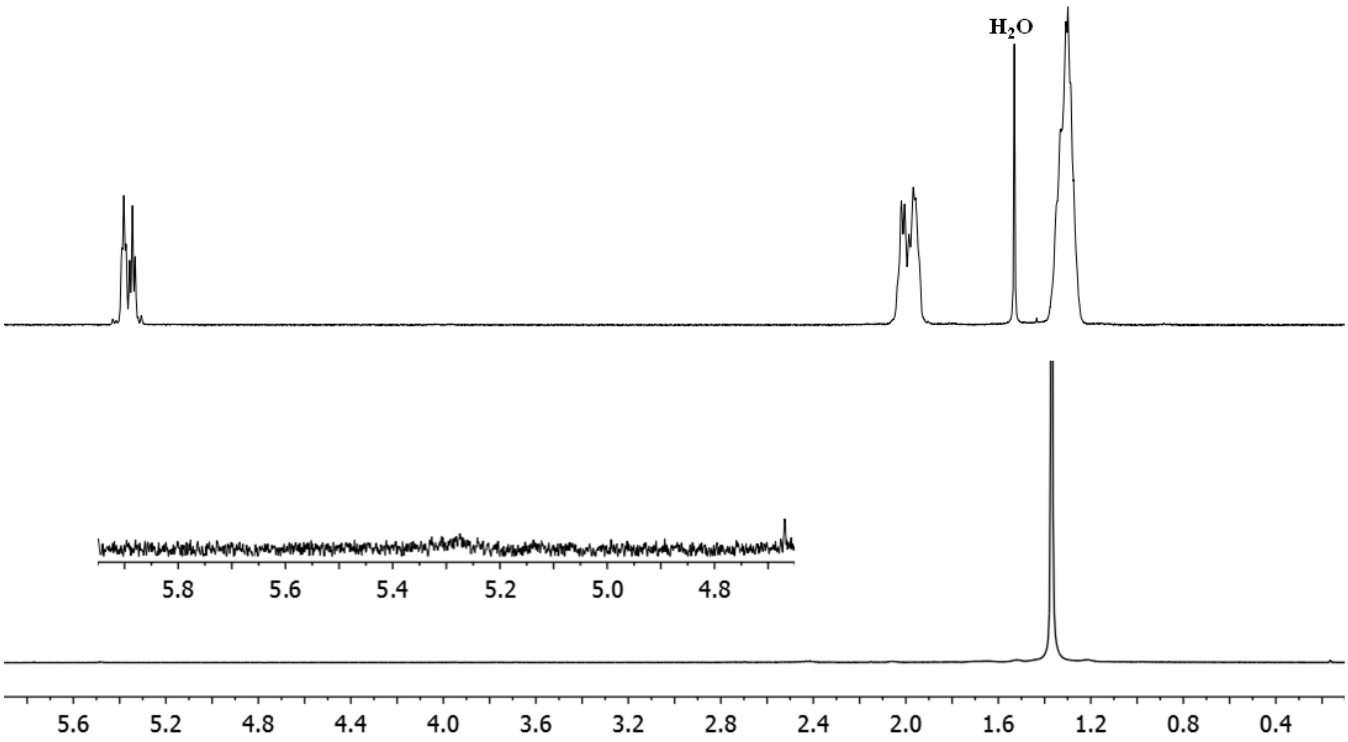

Figure S7. ^{1}H-NMR spectra of unsaturated polycyclooctene (top; 25 °C, $CDCl_3$; Table 1, entry 7) and after hydrogenation (bottom; 130 °C, $C_2D_2Cl_4$; Table 2, entry 3).

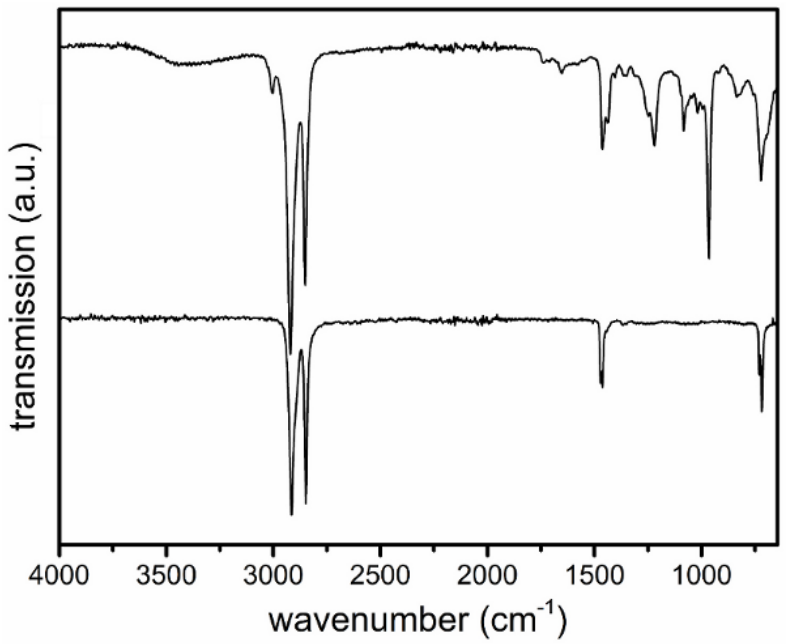

Figure S8. ATR-IR spectra of unsaturated polycyclooctene (top; Table 1, entry 7) and after hydrogenation (bottom; Table 2, entry 3).

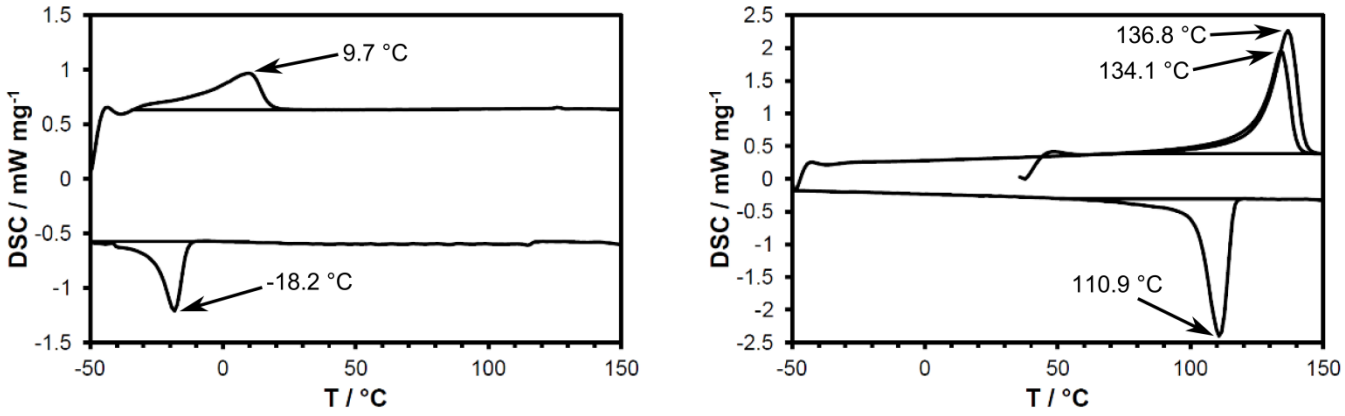

Figure S9. DSC traces of unsaturated polycyclooctene (left; Table 1, entry 3) and after hydrogenation (right; Table 2, entry 1).

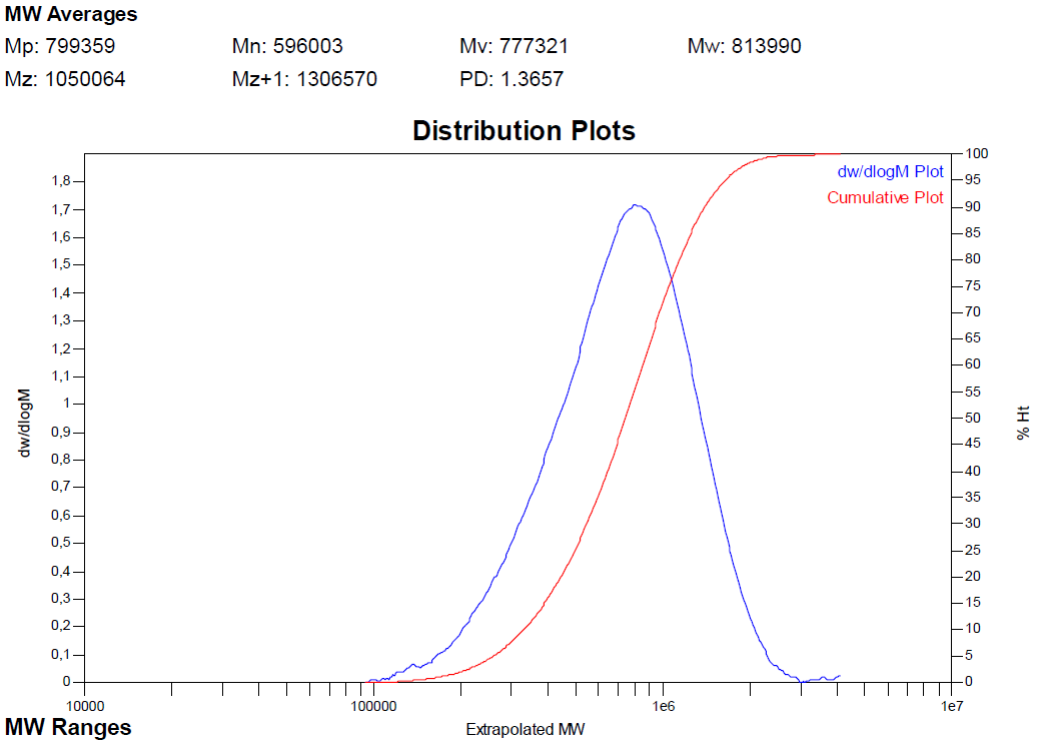

Figure S10. GPC trace of polyethylene after hydrogenation (Table 2, entry 1; TCB, 160 °C, vs. PE standards).

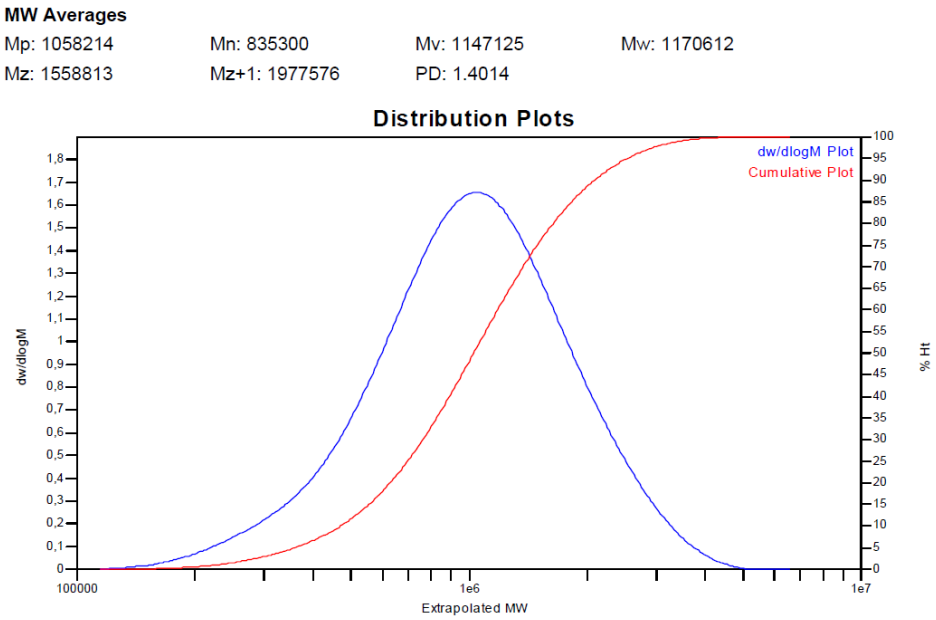

Figure S11. GPC trace of polyethylene after hydrogenation (Table 2, entry 2; TCB, 160 °C, vs. PE standards).

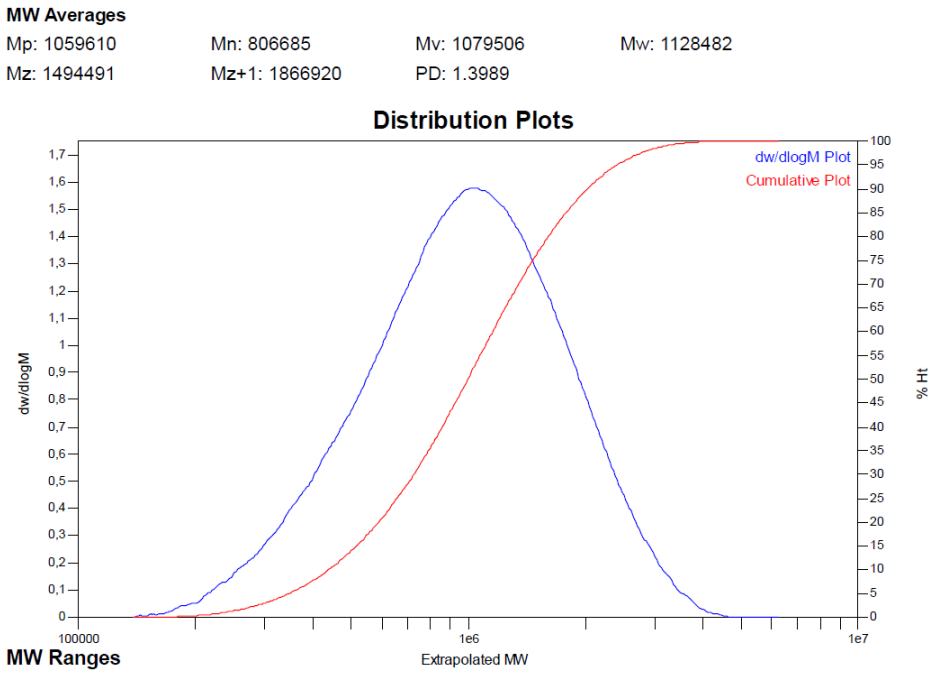

Figure S12. GPC trace of polyethylene after hydrogenation (Table 2, entry 3; TCB, 160 °C, vs. PE standards).

5. AFM studies

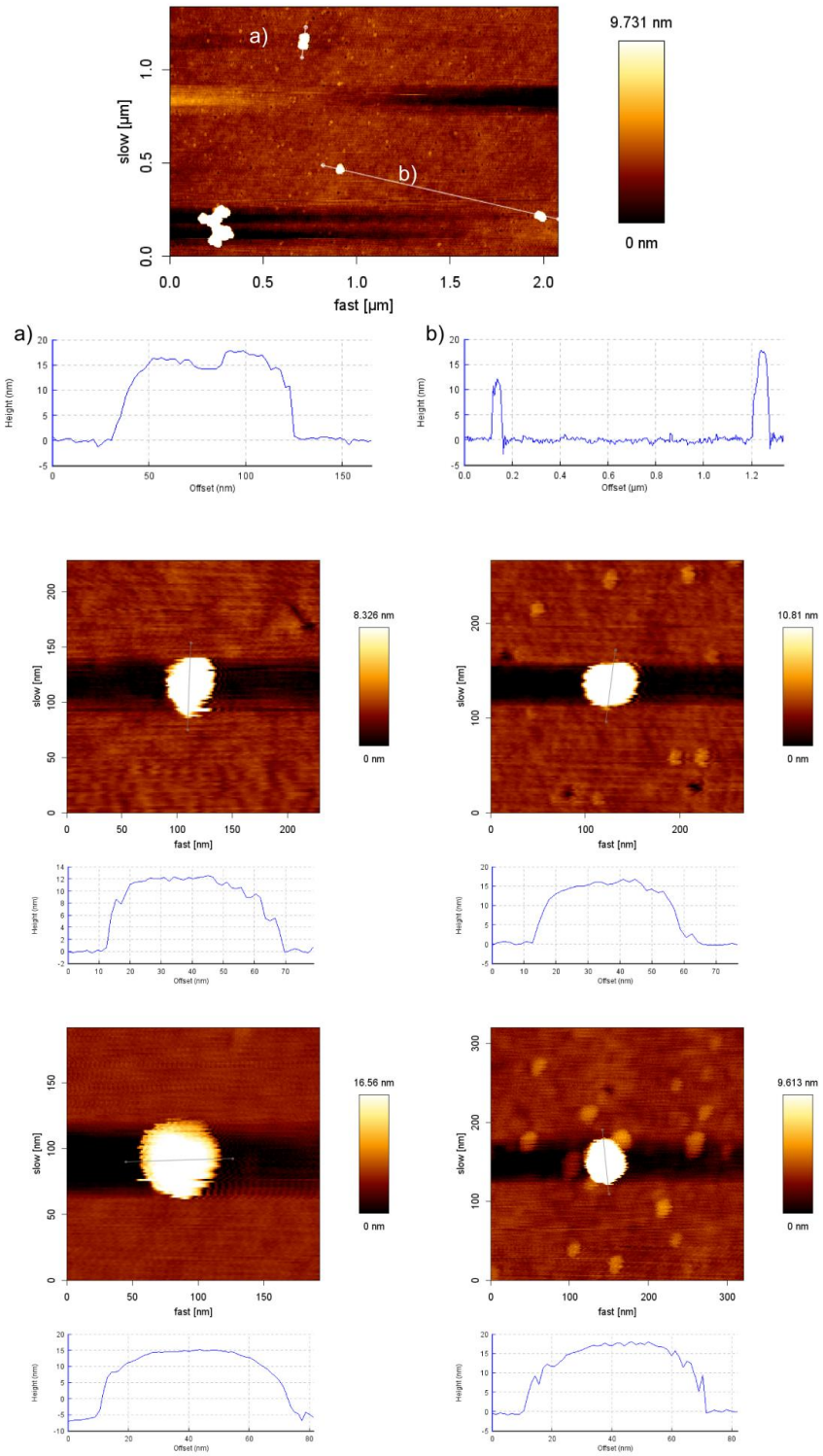

Figure S13. AFM height images of single fluorescence labeled PE nanocrystals **NP-1** (Table 2, entry 3) spincoated on a glass substrate and corresponding height cross sections.

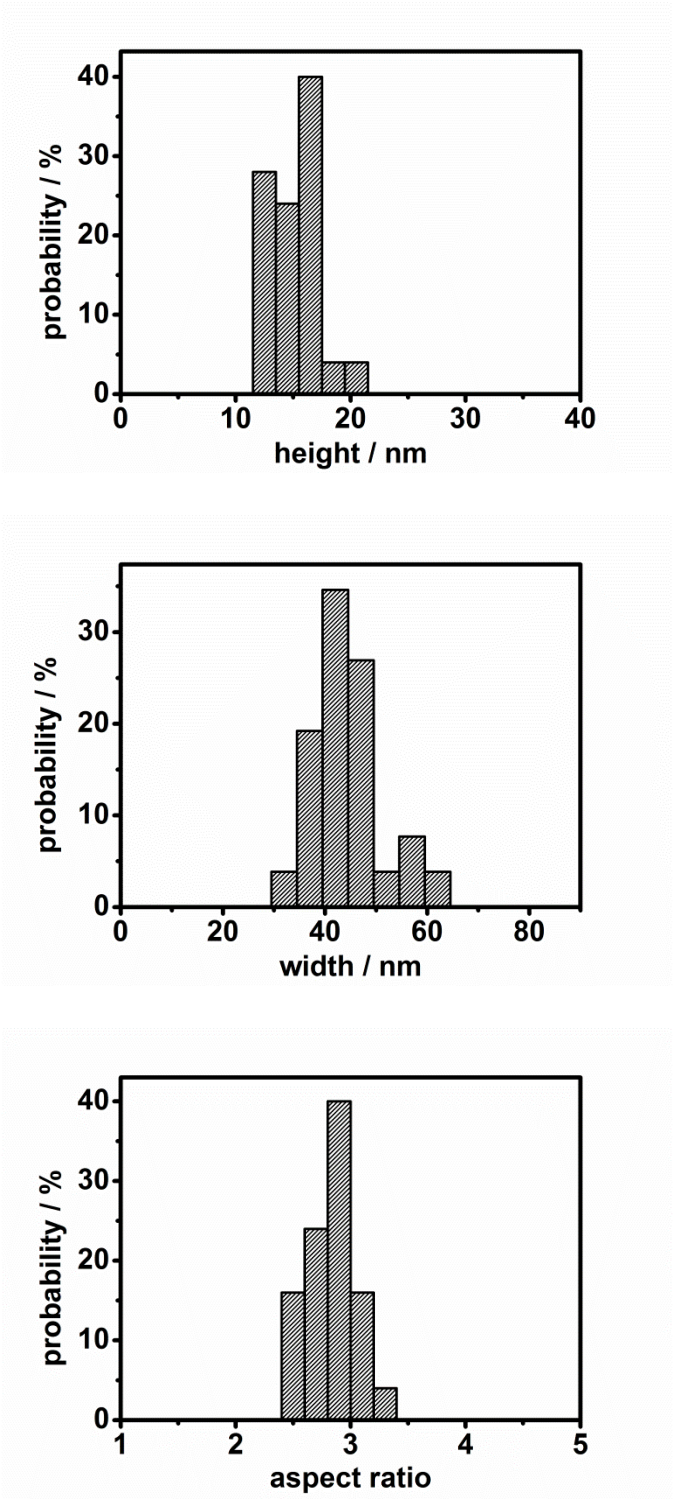

Figure S14. Histograms of the height (top), width (middle) and the aspect ratio (bottom) of single fluorescence labeled PE nanocrystals **NP-1** spincoated on a glass substrate determined by AFM.

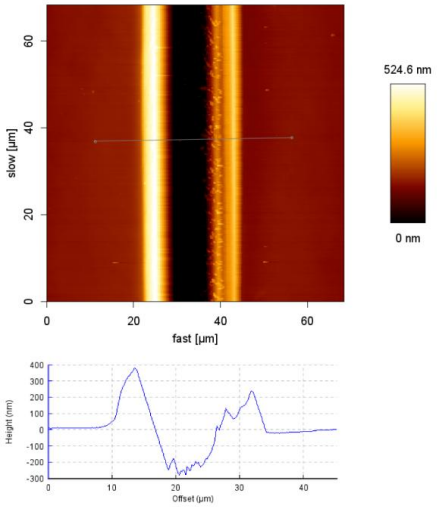

Figure S15. AFM height image of a PVA film with embedded single fluorescence labeled PE nanocrystals **NP-1** (top; Table 2, entry 3) and corresponding height cross section (bottom).

7. Defocused widefield images

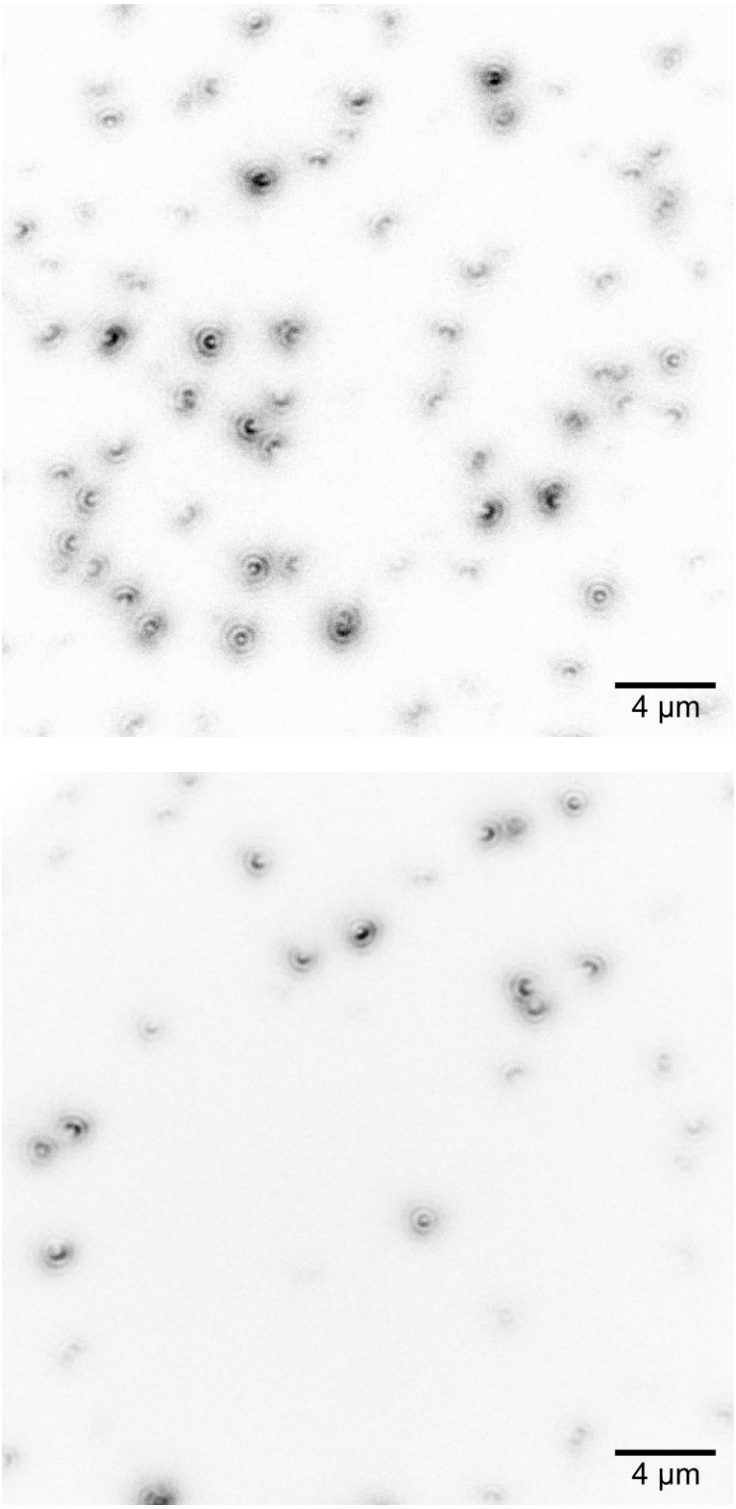

Figure S16. Typical defocused widefield images of **NP-1** (Table 2, entry 3) spincoated on a glass substrate.

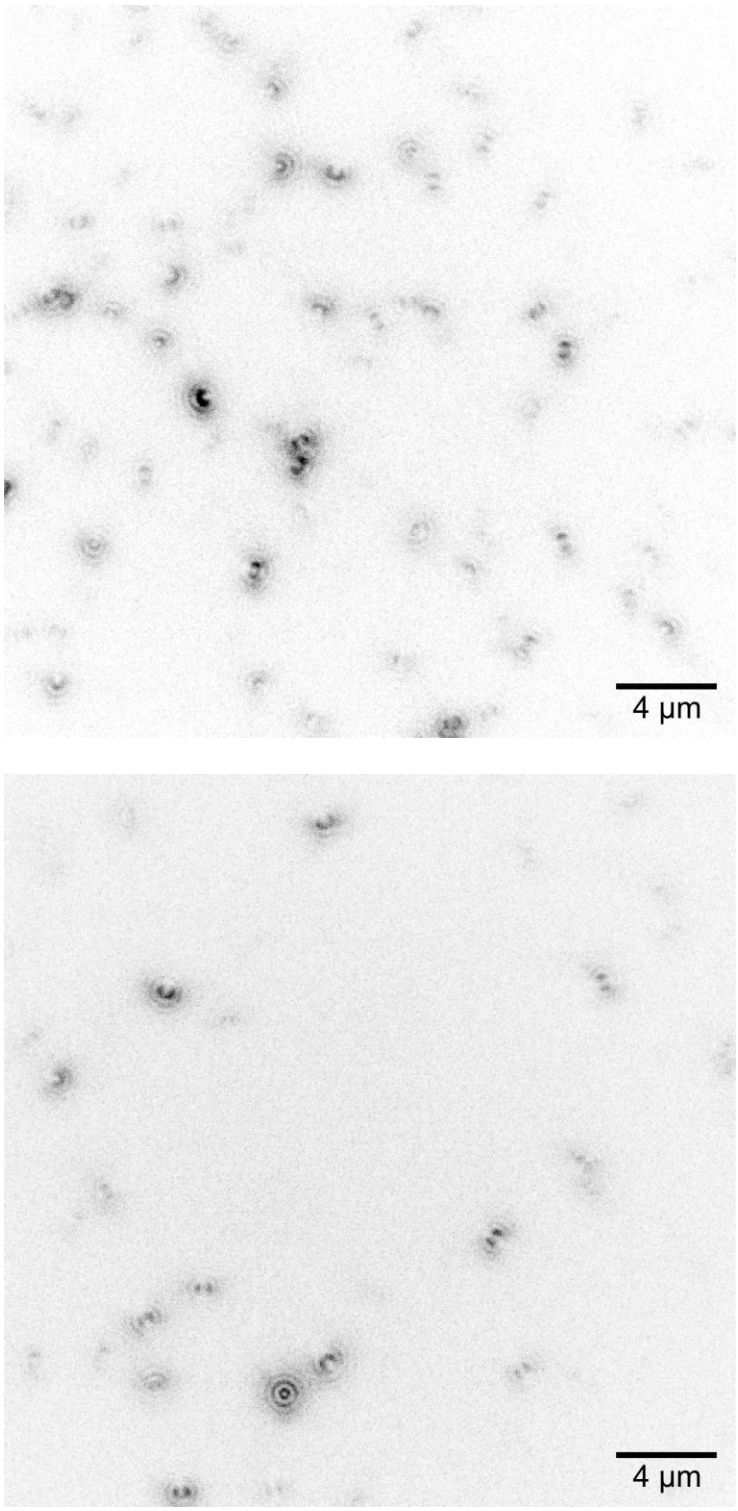

Figure S17. Typical defocused widefield images of **NP-1** (Table 2, entry 3) embedded in a 50–300 nm thick PVA matrix.

The probability of a statistically oriented molecule to possess an orientation in a range of a ≤ θ ≤ b was calculated by:

$$P = \int_a^b \sin\theta \, \mathrm{d}\theta \qquad \text{(eq 4)}$$

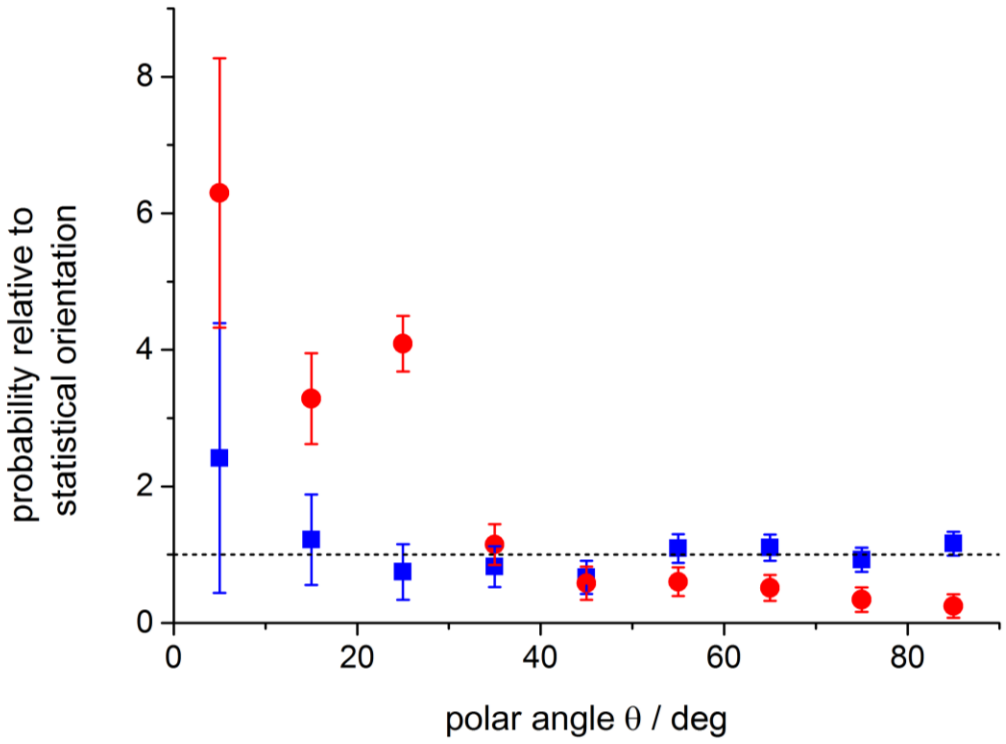

Figure S18. Ratio between the probabilities for the out-of-plane angle θ determined for the transition dipole moment of reporter molecules incorporated into the PE nanocrystals **NP-1** (red circles: **NP-1** spincoated on a glass substrate; blue squares: **NP-1** embedded in a PVA matrix) and expected for randomly oriented molecules. In the case of the PE nanocrystals lying flat on the substrate, the probability of the incorporated PDI dye molecules to possess an orientation of their transistion dipole moments with an out-of-plane angle of <30° is approximately 4-fold increased compared to randomly oriented dye molecules.

References

(S1) Oberhauser, T. *J. Org. Chem.* **1997**, *62*, 4504.

(S2) Rix, D.; Clavier, H.; Coutard, Y.; Gulajski, L.; Grela, K.; Mauduit, M. *J. Organomet. Chem.* **2006**, *691*, 5397.

(S3) Baggerman, J.; Jagesar, D. C.; Vallée, R. A. L.; Hofkens, J.; De Schryver, F. C.; Schelhase, F.; Vögtle, F.; Brouwer, A. M. *Chem. Eur. J.* **2007**, *13*, 1291.

(S4) Ego, C.; Marsitzky, D.; Becker, S.; Zhang, J.; Grimsdale, A. C.; Müllen, K.; MacKenzie, J. D.; Silva, C.; Friend, R. H. *J. Am. Chem. Soc.* **2003**, *125*, 437.

(S5) Pschirer, N. G.; Eickemeyer, F.; Schöneboom, J.; Qu, J.; Könemann, M.; Müllen, K.; Li, C.; Herrmann, A.; Erk, P.; Nordmann, G.; Kuhn, A.; Hagfeldt, A.; Edvinsson, T. (BASF AG) PCT Int. Appl. WO 2007/054470 A1, May 18, 2007.

(S6) Vougioukalakis, G.; Grubbs, R. *Chem. Eur. J.* **2008**, *14*, 7545.